Journal of Atmospheric and Solar-Terrestrial Physics 102 (2013) 243–251

Contents lists available at ScienceDirect

# Journal of Atmospheric and Solar-Terrestrial Physics

journal homepage: www.elsevier.com/locate/jastp

# Quantifying the importance of galactic cosmic rays in cloud microphysical processes

Akhilesh. Rawal [a], Sachchida Nand. Tripathi [a,*], Marykutty. Michael [a], Atul K. Srivastava [b], Richard G. Harrison [c]

[a] Department of Civil Engineering, Indian Institute of Technology, Kanpur, India
[b] Indian Institute of Tropical Meteorology (Branch), Prof Ramnath Vij Marg, New Delhi, India
[c] Department of Meteorology, University of Reading, UK

ARTICLE INFO

*Article history:*
Received 8 January 2013
Received in revised form
12 April 2013
Accepted 31 May 2013
Available online 13 June 2013

*Keywords:*
Aerosol charging
Cloud formation
Droplet growth
GCR flux

ABSTRACT

Galactic Cosmic Rays are one of the major sources of ion production in the troposphere and stratosphere. Recent studies have shown that ions form electrically charged clusters which may grow to become cloud droplets. Aerosol particles charge by the attachment of ions and electrons. The collision efficiency between a particle and a water droplet increases, if the particle is electrically charged, and thus aerosol-cloud interactions can be enhanced. Because these microphysical processes may change radiative properties of cloud and impact Earth's climate it is important to evaluate these processes' quantitative effects. Five different models developed independently have been coupled to investigate this. The first model estimates cloud height from dew point temperature and the temperature profile. The second model simulates the cloud droplet growth from aerosol particles using the cloud parcel concept. In the third model, the scavenging rate of the aerosol particles is calculated using the collision efficiency between charged particles and droplets. The fourth model calculates electric field and charge distribution on water droplets and aerosols within cloud. The fifth model simulates the global electric circuit (GEC), which computes the conductivity and ionic concentration in the atmosphere in altitude range 0–45 km. The first four models are initially coupled to calculate the height of cloud, boundary condition of cloud, followed by growth of droplets, charge distribution calculation on aerosols and cloud droplets and finally scavenging. These models are incorporated with the GEC model. The simulations are verified with experimental data of charged aerosol for various altitudes. Our calculations showed an effect of aerosol charging on the CCN concentration within the cloud, due to charging of aerosols increase the scavenging of particles in the size range 0.1 μm to 1 μm.



## 1. Introduction

Water vapor is an important, but variable, atmospheric constituent, and Earth's water cycle is mostly dependent on the formation and condensation of clouds. Small variations in cloud have the potential to influence the climate, therefore the suggestions that there are effects of galactic cosmic rays (GCR) on clouds (Hiremath, 2006; Gray et al., 2010) raise the question of how large the effects would be for the climate system. The GCR varies on many timescales, and, notably, with the Schwabe cycle of solar activity. Ion production in the lower and middle atmosphere is mostly governed by the GCR flux (Bazilevskaya et al., 2008) except very close to the surface of Earth, where surface release of radon also contributes. Particles on which clouds form-so called cloud condensation nuclei (CCN)—have been suggested to show, in some circumstances, sensitivity to ion production rates (Carslaw et al., 2002) as studies have shown that ions can form aerosols (Kulmala et al., 2004; Kirkby et al., 2011). If alternatively or additionally, CCN become electrically charged, the collision efficiency between a particle and a water droplet increases, which enhances aerosol-cloud interaction rates (Tripathi et al., 2006). Formation and growth of droplet from water vapor is directly related to supersaturation vapor pressure and distribution of particles within the cloud (Nenes et al., 2001). A cloud microphysical model has been developed, which includes electrically-influenced processes (Rycroft et al., 2012; Harrison and Ambaum 2008) and then coupled with a Global Electric Circuit (GEC) model. This coupled model was then used to study the correlation of GCR variation during the solar cycle to CCN concentration and the subsequent droplet distribution.

* Correspondence to: Department of Civil Engineering, Indian Institute of Technology Kanpur, Kanpur, UP – 208016, India.Tel.\fax: +91 512 259 7845.
E-mail addresses: snt@iitk.ac.in, mary@iitk.ac.in, gigimic@gmail.com (S.N. Tripathi).

1364-6826/$ - see front matter 
http://dx.doi.org/10.1016/j.jastp.2013.05.017

Five major models are included in the coupled simulation, which are (i) The prediction of cloud base, (ii)growth of cloud droplets, (iii) scavenging of particles within the cloud, (iv) electrical model within the cloud, and (v) GEC. One method for simulation of droplet growth and distribution in non-precipitating clouds is a cloud parcel model, which considers the conservation of heat and moisture within the parcel and predicts growth of aerosols to CCN (Nenes et al., 2001; Seinfeld and Pandis, 2006). When a rising air parcel reaches the level of supersaturation, water vapor starts to condense on the CCN present. The CCN arise from the background aerosol present; the subsequent microphysical processes such as condensation/coagulation growth, breakup, and evaporation decide the droplet distribution.

Droplets undergo gravitational settling in clouds. Aerosols have negligible settling velocities compared to droplets, because of their smaller size (mass) and greater upward forces. Droplets capture aerosols during collisions causing removal of aerosol from clouds. The fraction of particles colliding with drop is termed as collision efficiency. Studies have found relatively greater collision efficiency for fine and coarse mode aerosols due to Brownian forces and inertial forces, respectively; but very low collision efficiency in accumulation mode (0.1–2.5 μm particle size). This region of low collision efficiency has long been known as the Greenfield gap (Greenfield, 1957), but recent studies have shown that inclusion of electrical effects significantly increase the collisions efficiency so as to fill in the Greenfield gap (Tinsley et al., 2000, 2006; Tripathi et al., 2006; Zhou et al., 2009). These considerations have been implemented in the particle scavenging model.

Charges on aerosols can affect CCN and Ice Forming Nuclei (IFN) concentrations in the cloud (Tripathi and Harrison, 2001; 2002; Kanawade and Tripathi, 2006). It is therefore important to know the charge distribution of aerosols and droplets within the cloud. The vertical electric field within the cloud also plays a crucial role in charging process, as it establishes vertical motion of ions from one layer to other. Accumulation of opposite charges at the upper and lower edges of layer clouds has been confirmed (Nicoll and Harrison, 2010). Several numerical models have been developed to calculate the electric field, ion concentration, and aerosol charge distribution within clouds (e.g. Zhou and Tinsley, 2007; Srivastava and Tripathi, 2010).

Atmospheric air, due to the presence of small ions generated by cosmic rays, is always slightly electrically conductive. These small ions are highly mobile and can be accelerated easily under the existing electric field in the atmosphere. The magnitude electric field present in atmosphere varies from 100 $Vm^{-1}$ in fair weather to 10,000 $Vm^{-1}$ in thunderstorm (MacGorman and Rust, 1998). The global electric circuit is a combination of the upward current during thunderstorms and a very small compensating downward electric current during fair weather conditions (Harrison, 2000). For an aerosol-free atmosphere this field is small but can have certain impact on microphysical properties of clouds.

Models have been developed dealing with growth of droplets in the cloud (Nenes et al., 2001), collision efficiency of charged aerosol (Tinsley et al., 2006), and charging of aerosols in clouds (Zhou and Tinsley, 2007). All these models used mono-disperse distribution of aerosols and single charge on the particles. In the present work poly-disperse distribution of aerosols with multiple charge on the particles have been used, which is a more realistic scenario. For the first time, all these modeling approaches have been coupled together to study the effect of the variation of GCRs from solar minimum to maximum on cloud drop formation in stratiform clouds.

## 2. Model description

An integrated numerical model system has been designed to link aerosol charging, CCN formation, cloud growth, particle scavenging in the cloud, and GEC. This model is built from five different numerical models (given in Sections 2.1 to 2.5), coupled together. The flow diagram of the coupled model is provided in Fig. 1.

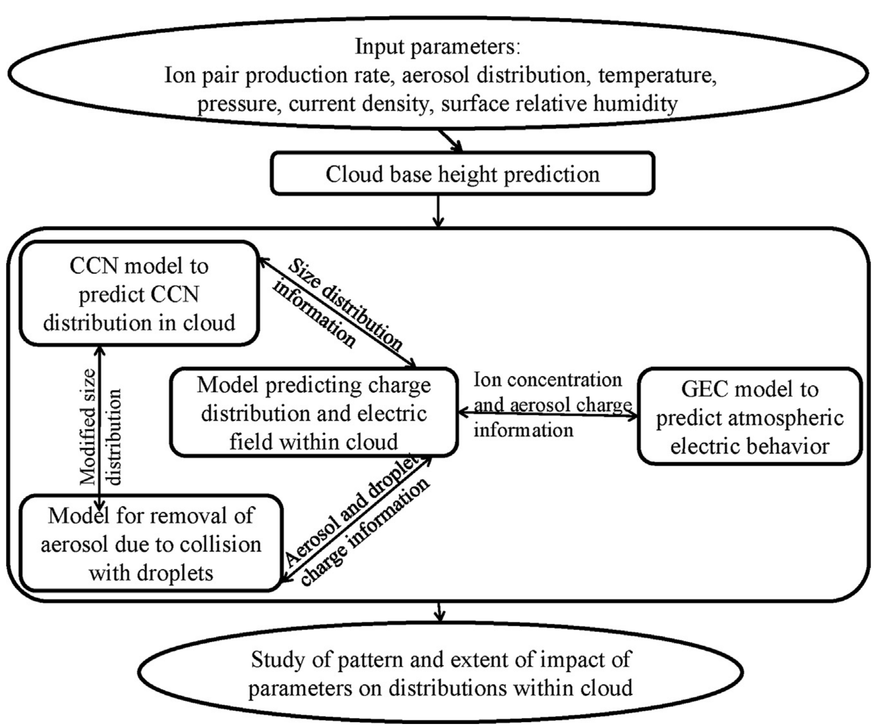


**Fig. 1.** Schematic diagram of different processes simulated by the coupled model approach adopted.

### 2.1. Cloud base prediction

For cloud base to be calculated, the required input parameters are surface temperature ($T$), pressure ($p$) and relative humidity ($RH$). The temperature of the cloud parcel decreases with height at the dry adiabatic lapse rate. When the temperature of the parcel reaches the dew point temperature air saturates at that altitude and cloud formation begins. The temperature at saturation is termed the isentropic condensation temperature ($T_{ICT}$), calculated by an iterative (Newton-Raphson) method as given in Eq. (1) (Jacobson, 1999),

$$T_{ICT} = \frac{4880.357 - 29.66\ \ln[w_v p/\varepsilon (T_{ICT}/T_0)^{1/\kappa}]}{19.48 - \ln[w_v p/\varepsilon (T_{ICT}/T_0)^{1/\kappa}} \quad (1)$$

where $w_v$ is the water vapor mixing ratio, which is constant until saturation reached. $w_v$ is calculated using relative humidity at the surface. $\varepsilon$ is the mass fraction of soluble material. After calculation of $T_{ICT}$, cloud base is predicted using Eq. (2).

$$\tau = \frac{dT}{dz} = -\frac{g}{c_p} \quad (2)$$

where $\tau$ is dry adiabatic lapse rate, $z$ is the base of the cloud, $g$ is gravity and $c_p$ is the specific heat of water, which is obtained from Seinfeld and Pandis (2006). This $\tau$ is then used to find out the altitude at which $T_{ICT}$ occur.

### 2.2. Particle growth model

This model starts with the assumption that super saturation has been reached by an ascending adiabatic cloud parcel, i.e. one for which there is no transfer of heat or moisture between the parcel and surroundings. In the air parcel, some particles start growing with condensation and some start evaporating. The input parameters required for this model are temperature and pressure at the surface and within the clouds, initial super saturation, vertical air parcel velocity and particle distribution. Though theoretical working of the parcel model is similar to that described in Nenes et al. (2001), a different numerical approach has been developed to study the growth behavior and cloud formation mechanisms. Super saturation and particle size distribution at every time step can be studied using this model.

A logarithmic bin structure is used to represent the aerosol size distribution. For every size bin, equilibrium super saturation and particle growth parameters are calculated. Cloud super saturation, particle growth parameter and equilibrium super saturation drive the dynamics of growth of droplet. As the size of droplets change, a moving bin algorithm is used to keep track of droplets and its dry radius. In moving bin algorithm particles are distributed in bins according to initial particle size distribution (Jacobson, 1999). During the computation, the number concentration of particles does not change but the size changes which is represented by a new, larger or smaller size bins.

Every parameter in the calculation of super saturation and growth of droplet is interdependent, which requires an iterative procedure to obtain a self-consistent solution of all of the parameters. Differential equations for growth of droplet and variation in concentration of water are solved by applying forward difference method. Equations for specific heat of water and latent heat of evaporation are solved every 10th time step because these quantities do not vary significantly for small changes in temperature. The steady-state particle size distribution calculated using this model has been validated against published results (Seinfeld and Pandis, 2006 (Figure 17.14); Andrejczuk et al., 2010; Jacobson, 2002).

### 2.3. Particle scavenging model

The collision efficiency (CE) is defined as the fraction of the particles within the volume swept out by a collector droplet which will actually collide with it (Tinsley et al., 2006; Zhou et al., 2009). CE is dependent on droplet radius ($A$), particle radius ($a$), droplet charge ($Q$), particle charge ($q$), density of particle ($\rho_p$), temperature ($T$), and pressure ($p$). Terminal velocity ($U$) is also required for the calculation, which is a function of radius, temperature and pressure. Collision efficiencies are used in the form of collision rate coefficients ($R$) in cloud models to evaluate scavenging of particles (Zhou et al., 2009). The number of particles scavenged per unit time per unit volume is calculated by multiplying $R$ with the concentrations of droplets and aerosols (Zhou et al., 2009). The present model was developed following the theory discussed in detail in Tinsley et al. (2006) and Zhou et al. (2009). Under steady state fair weather conditions the vertical current density is directed downward. This is the sum of downward current density due to the downward moving positive ions and the downward current density due to the upward moving negative ions. A positive space charge region is generated close to the upper boundary of the cloud and a negative space charge region is in the lower boundary of the cloud. Therefore, the derivative of the electric field is positive in the upper boundary layer and is negative in the lower boundary layer. In addition to that it has been improved by adding the effect of external electric field on collision efficiency in the present work as given in Eqs. (3) and (4). Here gravitational and external electric fields (E) are assumed to be aligned in the same direction.

$$\frac{\Delta r}{\Delta t} = \frac{B_p\left[F_e + F_{th} + F_{df} + (mg + qE)\cos\ \theta\right] + u_{r,pp}}{A} \quad (3)$$

$$\frac{\Delta \theta}{\Delta t} = \frac{u_{\theta,pp} - (\sin\ \theta/r)B_p(mg + qE)}{A} \quad (4)$$

here $r = b/A$, where b is the distance between the center of the droplet to the center of the particle. $\theta$ is angle between direction of movement of droplet and line joining centers of droplet and particle. The forces acting on the particle are electrical force ($F_e$), thermophoretic force ($F_{Th}$), diffusophoretic force ($F_{Df}$), and weight of particle ($mg$). $u_\theta$ and $u_r$ are the tangential and radial velocities of the droplet. The calculations use values similar to those of Tinsley et al. (2006) and Zhou et al. (2009).

The horizontal distance between the center of the particle to the center of the droplet is calculated as $x = r\sin\theta$. In this model, the initial ratio ($r$) is taken as 12. i.e. the initial radial distance between the droplet and the particles is 12 times the radius of the droplet. Here bracketing method is used with minimum width of bracket taken as 0.0001. Initial bracket for $x$ is taken as [0, 20]. In this run 42 exponential bins with a multiplicative factor of 1.3 and initial bin size 0.001 μm for size distribution of aerosol have been used. Collision occurs when r≤1, and collision stops when r >14. As radius increases, particle inertia becomes comparable to electric forces and for denser particles collision efficiency decrease. For particles of very small radius, collision efficiency decreases because they do not follow the stream function due to their small inertia.

Simulated results are in agreement with the published results (Tinsley et al., 2006). With increasing electric field, collision efficiency of smaller particles decrease but for larger particles the effect is negligible (Fig. 2). Movement of smaller particles in stream flow is mostly governed by electric force because of smaller mass inertia force is almost negligible, but for larger particles, the movement is governed by inertia as electric force is very small due to higher mass.

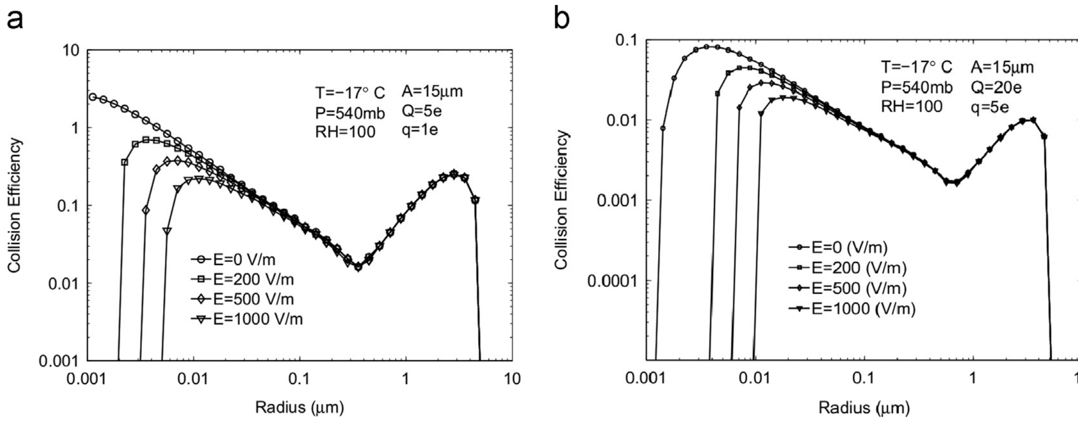


**Fig. 2.** Collision efficiency for different external electric field. (a) Charge on droplet ($Q$)=5e and on particle ($q$) =1e. Droplet radius is 15 μm (b) Charge on droplet ($Q$)=20e and on particle ($q$) =5e.

**Table 1**
Collision efficiency ($m^3\,s^{-1}\times10^{-14}$) for droplet radius 30 μm and particle radius 1 μm.

| Droplet charge | Particle charge | | | | |
|---|---|---|---|---|---|
| | 0e | 1e | 2e | 4e | 8e |
| 0e | 115.35 | 116.37 | 116.37 | 117.29 | 120.50 |
| 80e | 115.35 | 116.37 | 116.37 | 117.29 | 120.50 |

**Table 2**
Collision efficiency ($m^3\,s^{-1}\times10^{-14}$) for droplet radius 30 μm and particle radius 0.3 μm.

| Droplet charge | Particle charge | | | | |
|---|---|---|---|---|---|
| | 0e | 1e | 2e | 4e | 8e |
| 0e | 7.60 | 10.59 | 21.12 | 50.13 | 112.52 |
| 80e | 7.60 | 10.59 | 21.12 | 49.42 | 111.47 |

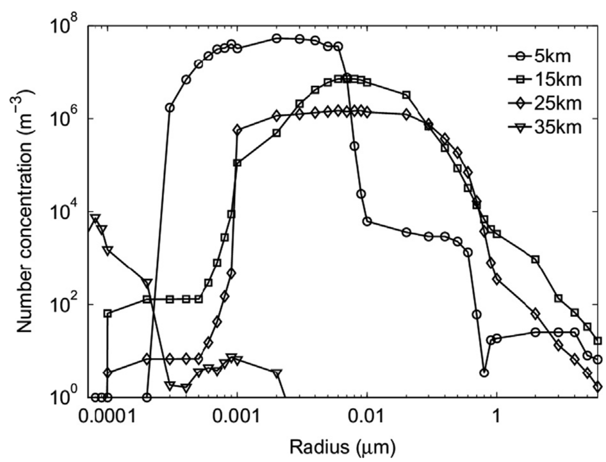


**Fig. 3.** Observed particle size distributions at various altitudes. The distribution at 5 km is from Zaizen et al. (1995), at 15 and 25 km from Zhau et al. (1995), and at 35 km from Yu and Turco (2001).

Simulations were done to study the impact of charges on droplets and aerosols on collision efficiency. Table 1 and 2 show the collision efficiency calculated for particle sizes 1 μm and 0.3 μm, respectively. Though the effect of droplet charge on the collision efficiency is negligible, charges on the particles have a significant effect.

## *2.4. Global electric circuit (GEC) model*

A small "fair weather" current density flows from ionosphere to Earth's surface due to the potential difference between the surface and the ionosphere. This potential difference is sustained by high current flow in disturbed weather regions, such as shower clouds and thunderstorms. The entire process of current flow is termed as global electric circuit. A model has been developed to study the current density ($J_z$) flowing downward from the ionosphere to the surface. The atmospheric conductivity variation, principally varying in the vertical, needs to be understood to study the global electric circuit. The atmospheric conductivity is a function of the concentration of the ions and their mobilities (Tinsley and Zhou, 2006; Tripathi et al., 2008; Michael et al., 2008; 2009). The long-lived ion clusters contribute mostly to the atmospheric conductivity. The ions become attached to aerosols and transfer the charge to the aerosols. The steady-state ion and aerosol concentrations are calculated using charge balance equations and the details are provided in Tinsley and Zhou (2006), Tripathi et al. (2008), and Michael et al. (2008; 2009). After the steady-state ion concentrations are calculated the conductivity of the atmosphere is calculated and subsequently, the resistivity and columnar resistance of the atmosphere, and the current density are calculated as described in Tinsley and Zhou (2006).

In the GEC model, an upper vertical limit of 45 km is used with a bin size of 1 km. The production of ions due to GCR is affected by the magnetic field and the solar flux. The model developed by K. O'Brien. (PLOTINUS (Programmed Linear Operator for the Transport of NUclear Showers) (O'Brien, 2005)), can calculate the ion-pair production rate by statistical interpolation using experimental data at different altitude, latitude, longitude and time. The ion production rate is calculated using the model PLOTINUS (O'Brien, 2005) in the present work. The most abundant ion clusters considered in the model are ($SO_4^{2-}$) and ($NH_4^+$). Ionic mobility and mean free path are calculated using the expression from Borucki et al. (1982). The aerosol size distribution for this GEC model is taken from experimental data published in Yu and Turco (2001), Zhau et al. (1995), and Zaizen et al. (1995). Experimental data is available only for four altitudes and Fig. 3 shows the aerosol number distributions at these 4 altitudes. Renard et al. (2008; 2010) provide altitude profiles for aerosols of different sizes up to the stratosphere. To obtain size distribution for all altitudes for the model, a Gaussian vertical profile is created, centered on each altitude. Such aerosol distribution may vary substantially very close to the inversion layers, but in the present study concerning cloud base at 5.5 km and the aerosol size distribution is less variable. To represent the poly-disperse distribution, the size range of the aerosols is divided into 42 bins beginning from 0.001 μm with a multiplicative factor of 1.3. Ion-aerosol attachment coefficients are calculated as discussed in Michael et al. (2008; 2009) and Tripathi et al. (2008), which is based on the theory developed by Hoppel and Frick (1986). The GEC model results have been validated against published results (Tinsley and Zhou, 2006), and experimental results where they are available (Renard et al., 2013).

### 2.5. Electrical model within clouds

Clouds are integral part of global electric model. The electrical processes in cloud differ from those in clean air due to the presence of droplets which remove ions by attachment. The downward current density $J_z$ from the ionosphere to the surface of the planet generates space charge at the upper and lower boundaries of layer clouds (Rycroft et al., 2012; Srivastava and Tripathi, 2010). The droplet concentration is made zero at both the edges of the cloud, between which the droplet concentration increases to, where there is a layer of cloud with maximum droplet concentration. The ion concentration decreases to a minimum in the interior of the cloud as these ions get attached to the cloud droplets. As the ion concentration is at its minimum in the interior of the cloud, the electric field attains a maximum value. As the variation of concentration of droplets vary only in the upper and lower boundary layers of the cloud, this model can be applied to a cloud with a different interior thickness. The conductivity within the cloud is reduced by about an order of magnitude compared to that of the clean air at the same altitude because of the attachment of the ions to the cloud droplets (Zhou and Tinsley, 2007). As the current density flows through the boundaries of the cloud, it creates a gradient in electric field because of the gradient in conductivity between the cloud and the clean air. Incidentally the electric field gradient involves the generation of space charge (Zhou and Tinsley, 2007). The charge distribution on the aerosols and droplets, the conductivity and the electric field within the cloud are calculated, as discussed in Zhou and Tinsley (2007). Poly-disperse distribution of aerosols and droplets are used here and these are able to acquire multiple charges, which is an improvement of the model presented in Zhou and Tinsley (2007). Therefore the required modifications are made in the equations provided in Zhou and Tinsley (2007) to incorporate the poly-disperse distribution of aerosols and droplets.

The base of the cloud has been predicted using the method discussed in cloud base prediction model. The thickness of the cloud is arbitrary, but following Zhou and Tinsley (2007), it is considered here to be 35 m. The transition thickness from cloudy to clean air is taken to be 10 m from both upper and lower cloud boundaries and 15 m is the middle layer with almost fully saturated cloud, although the thickness of middle region has little effect on value of electric field. The droplet distribution remains the same throughout the middle layer of the cloud. As the interior of the cloud is uniform, the results for the boundary layers are applicable to clouds with uniform middle layer and of any thickness. The height of the cloud has been divided in to 35 altitude bins of 1 m. The temperature, pressure, and aerosol distribution are taken from the altitude profile used in GEC model. Initially, aerosols and droplets are considered to be neutral. The poly-disperse distribution of droplets within the cloud is represented by 10 size bins with the initial bin size of 10 μm. The bin size increases in geometric progression with a multiplicative factor of 1.2. The droplet concentration variation with cloud depth is regarded as sinusoidal, with nodes at boundary and maximum value at middle of cloud. Typical values of ion pair production rate ($q$) and current density ($J_z$) are taken as $6 \times 10^6$ cm$^{-3}$ s$^{-1}$ and $3 \times 10^{-12}$ Am$^{-2}$ respectively (Harrison and Carslaw, 2003; Zhou and Tinsley, 2007).

The variation of droplet concentration on each layer within the cloud is an input parameter, and charge is conserved across the whole cloud. Layers can exchange ions which have negligible mass with respect to aerosol and droplet. It is assumed that there is no movement of droplet on the charging time-scales, hence mass for each layer is conserved. Charging of aerosols in one layer is dependent on another layer due to flow of ion within the layer by presence of electric field. Sensitivity analysis using clouds of different thickness (50,75 and 100 m) found little variation in the electric field found in the middle of cloud layer in agreement with the published results of Zhou and Tinsley (2007). Also, the value of electric field varies up to 5–7% when compared to the results of 1000 m deep cloud (Srivastava and Tripathi, 2010). A charge distribution is generated for poly-disperse particle, to enable this model to be coupled and used with scavenging and cloud growth model.

### 2.6. Inputs and assumptions

Surface temperature and pressure are taken from the U.S. standard atmosphere 1976. Saturation vapor pressure of water and terminal velocity was calculated using empirical formulas from Seinfeld and Pandis (2006). The droplet radius is allowed to vary between 6 and 100 μm, and the particle radius between 0.01 and 10 μm. The range of droplet charge ($Q$) and particle charge ($q$) are shown in Tables 1 and 2. The relative particle density was taken as 1.5, following a test of sensitivity in the range 1.0–1.9. All these input parameters are similar to those of Tinsley et al. (2006) and Zhou et al., (2009).

No horizontal movement of droplet due to wind effect is considered in calculation of collision efficiency, because, in stratus clouds, very little horizontal disturbance is expected. As the difference in mass between droplet and particle is large, it is assumed that the droplet path or velocity are unaffected by particle attachment. If the mass of droplet and particle are similar then the vertical velocity may vary and subsequently affect the collision efficiency calculation. After super saturation, adiabatic particle growth was assumed as energy transfer is mostly due to vertical temperature difference and there is no horizontal temperature difference in close vicinity. The model is intended to represent fair weather conditions and one dimensional conduction current flows in vertically downward direction with negligible horizontal flow.

### 2.7. Coupling of all models

All modules in the coupled model are linked with exchange of the information to each other at every time step. Coupling of models is done step wise to ensure integration and exchange of data is done properly. It also helps in checking the accuracy of model at every step of coupling.

Initially, cloud base is predicted, and then for every time step, charge distribution and modified aerosol distribution are calculated. Charging and electro scavenging effects form part of these calculations. The cloud charging model and GEC model are conceptually very similar, with the only difference being the presence of droplets and exchange of ions within layers in cloud model. Ion concentration and the conductivity vary due to the presence of droplets. Ion concentration and conductivity calculated from cloud model are utilized in GEC model as input. Boundary conditions on the ion concentration and electric field for the cloud are taken from results of GEC model.

The size distribution of particles is an input for the charging model. In every 30 s time-step, the size distribution data is extracted from particle growth model and used in charging model. As a moving bin method is used to simulate size distribution in the droplet growth model, charge distribution within a bin remains same. The value of ion-aerosol attachment coefficient ($\beta$) is calculated after every time step to account for the changed aerosol radius. Changes in $\beta$ due to change in temperature is negligible.

Collision efficiency is included in this model by implementation of electro-scavenging, following the method of Tinsley et al. (2006) and Zhou et al. (2009).Charge distribution and size distribution are inputs to the scavenging model, both of which are found from the charging model and growth model, respectively. Due to scavenging of particles, both size and charge distribution change, and new size distribution from scavenging are used in growth model for further computations. Each model exchanges data after every 30 s computation, transferring its output parameters to the next model.

## 3. Results and discussion

To understand the pattern of droplet growth and validate it against Seinfeld and Pandis (2006), the initial distribution and the particle distribution at various growth stages are plotted in Fig. 4. It is shown that the particle grows very rapidly in the beginning and then the growth rate slows. This is in agreement with Seinfeld and Pandis (2006), that the particles grow rapidly until they reach a certain radius and then all particles follow almost similar steady growth rate further.

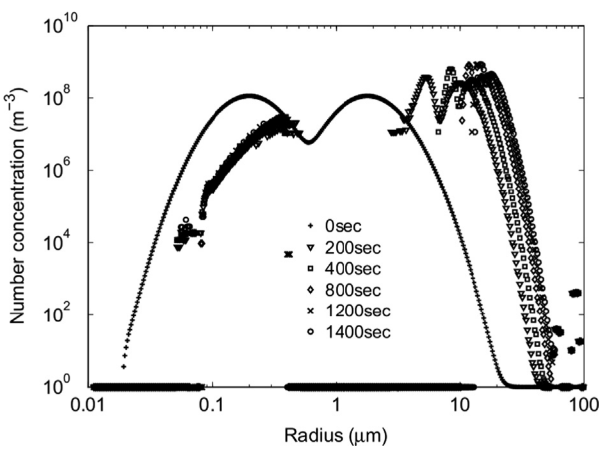


**Fig. 4.** Evolution of the particle size distribution. (Initial particle distribution is a multi log normal distribution, with means at 0.002 μm and 0.7 μm).

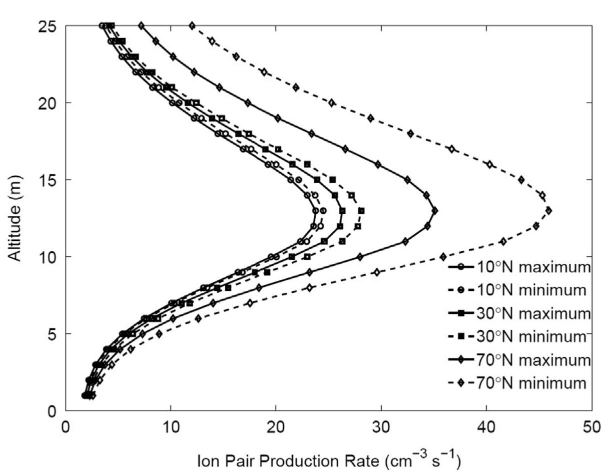


**Fig. 5.** Ion pair production rate for different solar flux values and for different latitudes. The model from O'Brien (2005) has been used to calculate the ion pair production rate.

To study the effect of GCR on the particle distribution within the cloud, the ion production rates typical for the usual range of solar activities across the solar cycle are calculated. Fig. 5 shows the ion production rate calculated for solar maximum and minimum for different latitudes (10°, 30° and 70° N). These GCR generated ions show a peak in production rate at an altitude of 12 km. At this peak altitude, the production rate at solar minimum is about 20 to 30% more than that at solar maximum for 70° N. For other altitudes and latitudes the difference in ion production rate is much smaller.

Figs. 6 (a)and (b) show the charge distribution on particles at 20 km and 1 km in the atmosphere, respectively. Particles in the smallest size range (0.001–0.01 μm), carry only a single charge and larger particles carry upto $\pm 10$ charges. This is because the attachment coefficient increases with the radius of the particle and therefore larger particles can carry multiple charges compared to the very small particles. Charge dstribution on droplets within the cloud for different size range are shown in Fig. 6 (c). Paricles in the smallest size range (0.01–0.1 μ m) carry only 2 to 3 electronic charge and as the size increases, the particles carry more charges.

Fig. 7 shows the steady state ion concentration in the atmosphere for different solar activities and at different latitudes (10° and 70° N). Fig. 8 shows the atmospheric conductivity profile.

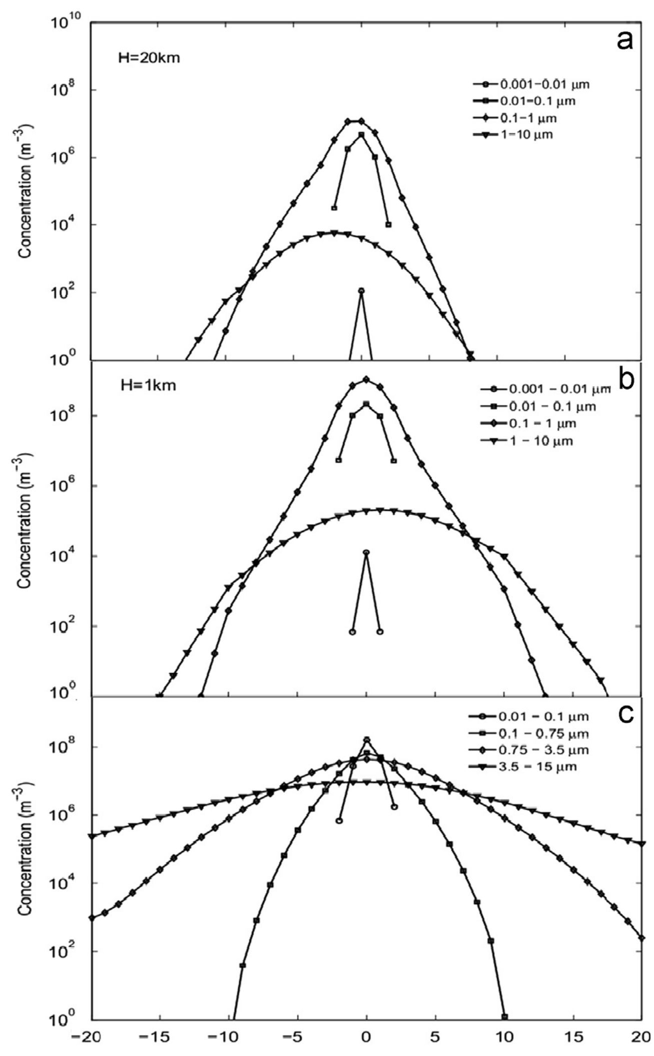


**Fig. 6.** Charge distribution of aerosols at (a) 1 km and (b) 20 km for different radius ranges and (c) Charge distribution on aerosols within the cloud for different size bins. Cloud base is at 4 km.

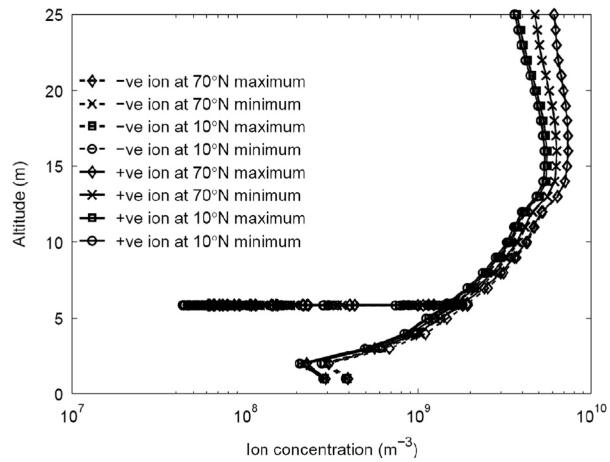


**Fig. 7.** The steady state ion concentration profile for different solar activities, at different latitudes. (Dashed line represents –ve ions and solid line represents +ve ions.).

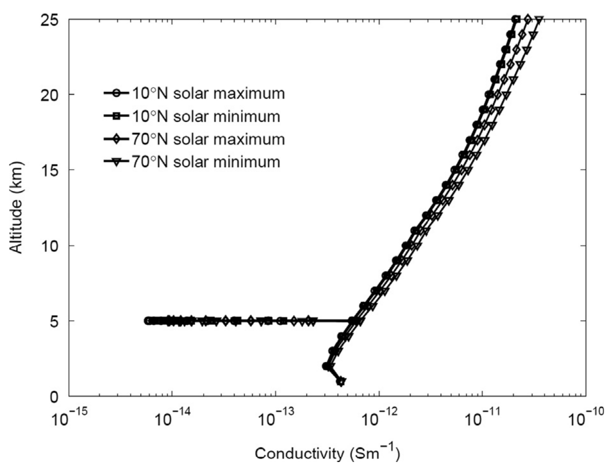


**Fig. 8.** Variation of electrical conductivity with altitude for different solar flux values and different latitudes.

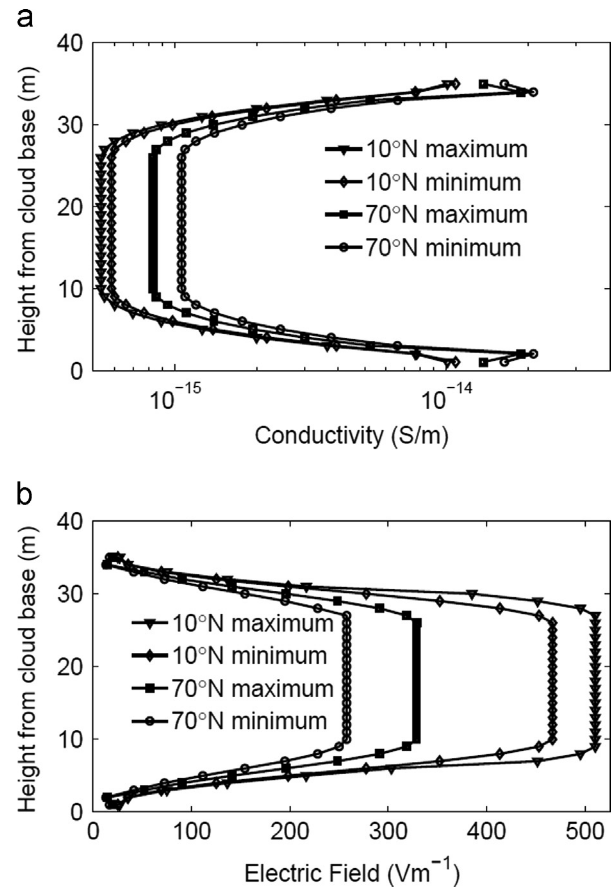


**Fig. 9.** (a) Variation of electrical conductivity within the cloud and (b) Electric field profile within the cloud for different solar flux values and for different latitudes.

There is very little variation in conductivity due to change in ion pair production, because, in clean air, ion–ion recombination almost compensates for the small changes in ion pair production rate, with conductivity variations dominated by variations in aerosol. The reduction in conductivity at about 5.5 km is due to the presence of the cloud.

The conductivity within the cloud is shown in Fig. 9(a). Variations of electric field within the cloud for different conditions are plotted in Fig. 9(b). The electric field is constant in the uniform part of the cloud and decreases to a minimum at the boundaries. The enhancement in electric field is due to the production of charged droplets associated with the ion removed within the cloud (Zhou and Tinsley, 2007; Srivastava and Tripathi, 2010) and it varies appreciable with both solar activity and latitude.

In the fully coupled model, the surface relative humidity is taken as 50%, following a sensitivity analysis which showed little variations as the surface humidity was varied between 30 and 80%. This choice also leads to a cloud base of around 5.5 km where the effect of surface ion pair production is negligible but the aerosol concentration remains sufficiently substantial to allow particle growth changes to be analyzed.

The distribution of particles 1500 s from initialization of model is plotted in Fig. 10(a). Results from three kinds of simulations are included in Fig. 10(a). In the first simulation, particle scavenging module is removed and therefore, only particle growth is calculated without accounting for scavenging removal. In the second simulation, particle growth and scavenging both are included, but the particles and droplets are neutral and therefore there is no electric force governing the movement of particles. The third simulation takes into account charges on the particles and droplets also. It is clearly shown in Fig. 10(a) that the charges on the particles have a significant effect in the distribution of particles in the Greenfield gap. That is, more particles in the accumulation mode are removed by scavenging, when charges on the particles are introduced.

Alkezweeny et al. (1993) reported the cloud droplet distribution at Denver, Colorado and Kansas City and found the mode diameter at about 10 to 15 μm. In-situ measurements of the microphysical properties of the warm stratocumulus cloud over maritime and continental region were carried out by Martin et al. (1994) and reported a mode diameter of 5 to 15 μm for droplets. Frisch et al. (1995) measured cloud droplet parameters over Portugal and found the mode diameter to vary from 4 to 12 μm. Henning et al. (2002) measured cloud droplet distribution during a field campaign at the high-alpine Jungfraujoch site and found a modal diameter of about 8 to 18 μm. Janssen et al. (2011) estimated the droplet concentration and the effective radii using MODIS data for the low-level stratiform clouds over the boreal forest and found that the effective radii of the droplets vary between 9 to 15 μm over different months. The mode diameter of the cloud droplets obtained from the present work is about 15 to 20 μm, similar to that reported elsewhere.

The steady state particle size distributions within the cloud at different solar conditions and at different latitudes are shown in Fig. 10(b). It can be seen that the distributions do not vary much with solar conditions or latitudes. The cloud base is predicted at

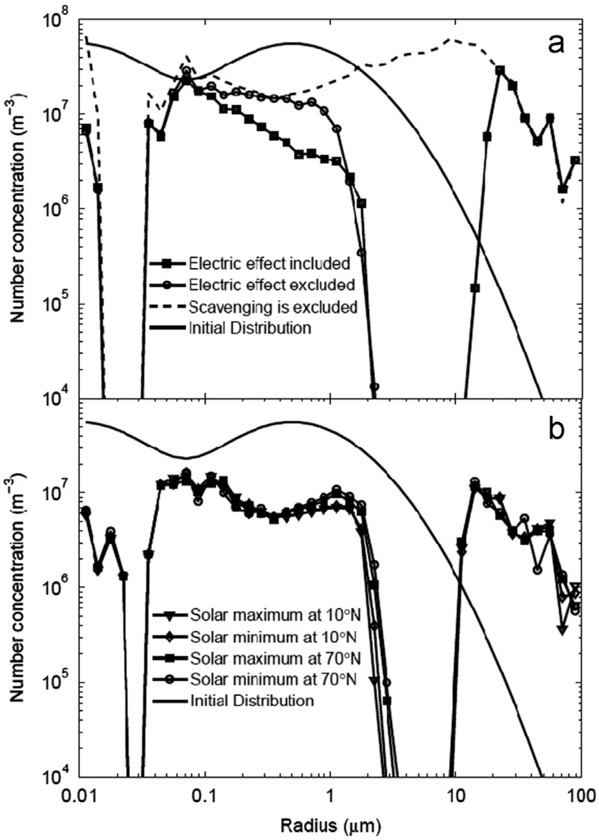


**Fig. 10.** (a) Particle size distribution at steady state (1500 s). Dashed line is the distribution, where particle growth is included and not the scavenging. Charges on the particles are excluded. Line with circles show the distribution, where growth and scavenging are included and the charges on the particles are excluded. The line marked with squares shows the distribution, where particle growth, scavenging and charge on the particles are included and (b) Particle size distribution at steady state (1500 sec) for different solar activity at different latitudes.

about 5.5 km and the thickness of the cloud is 35 m. The ion production rate at 5.5 km for different solar conditions is almost same and it explains the similarity in the particle distributions within the cloud.

## 4. Conclusion

Atmosphere dynamics is governed by several simultaneous physical processes. Electric effects also co-exist in cloud with the thermodynamics of droplet growth. In this study, the particle size distribution within cloud is calculated with only thermo-dynamical process, on which electrical phenomena are considered. Electric field and charging of aerosols have appreciable effects on the particle distribution. Results show differences in concentration up to a factor 3–5 for particle of radius 0.03–0.4 μm. Further significant concentrations of aerosols are found which carry up to 7e (elementary charges), exceeding the assumptions of previous work in which the aerosol charge has only been given unitary values (Tinsley et al., 2006).

Growth of particles due to super-saturation become slow after1500–2000 s, and most of the droplets gain size around 10–20 μm typical of in-situ measurements reported similar mode diameter of the cloud droplets as obtained in the present work. Further, for typical changes in local ionization associated with the GCR flux, small changes occur in the concentrations of sub-micron particles, but not in the resulting droplet size distribution.

## Acknowledgments

This work has been supported by the Ministry of Earth Sciences (MoES). MM acknowledges support through the DST Fast Track Fellowship. AKS acknowledges support and encouragement from the Director, IITM.

## References

Alkezweeny, A.J., Burrows, D.A., Grainger, C.A., 1993. Measurements of cloud droplet size distribution in polluted and unpolluted stratiform clouds. Journal of Applied Meterology 32, 106–115.

Andrejczuk, M., Grabowski, W.W., Reisner, J., Gadian, A., 2010. Cloud-aerosol interactions for boundary layer stratocumulus in the Lagrangian Cloud Model. Journal of Geophysical Research 115, D22214, http://dx.doi.org/10.1029/2010JD014248.

Bazilevskaya, G.A., Usoskin, I.G., Flückiger, E.O., Harrison, R.G., Desorgher, L., Bütikofer, R., Krainev, M.B., Makhmutov, V.S., Stozhkov, Y.I., Svirzhevskaya, A. K., Svirzhevsky, N.S., Kovaltsov, G.A., 2008. Cosmic ray induced ion production in the atmosphere. Space Science Reviews 137, 149–173, http://dx.doi.org/10.1007/s11214-008-9339-y.

Borucki, W.J., Levin, Z., Whitten, R.C., Keesee, R.G., Capone, L.A., Toon, O.B., Dubach, J., 1982. Predicted electrical conductivity between 0 and 80 km in the Venusian atmosphere. Icarus 51, 302–321, http://dx.doi.org/10.1016/0019-1035(82)90086-0.

Carslaw, K.S., Harrison, R.G., Kirkby, J., 2002. Cosmic rays, clouds, and climate. Science 298, 1732–1737, http://dx.doi.org/10.1126/science.1076964.

Frisch, A.S., Fairall, C.W., Snider, J.B., 1995. Measurement of Stratus cloud and drizzle parameters in ASTEX with a $K_\alpha$ band doppler radar and a microwave radiometer. Journal of the Atmospheric Sciences 52, 2788–2799.

Gray, L.J., et al., 2010. Solar influences on climate. Reviews of Geophysics 48 (RG4001), 53, http://dx.doi.org/10.1029/2009RG000282.

Greenfield, S., 1957. Rain scavenging of radioactive particulate matter from the atmosphere. Journal of Meteorology 14, 115–125, http://dx.doi.org/10.1175/1520-0469(1957)014%3c0115:RSORPM%3e2.0.CO;2.

Harrison, R.G., 2000. Cloud formation and the possible significance of charge for atmospheric condensation and ice nuclei. Space Science Reviews 94, 381–396, http://dx.doi.org/10.1023/A:1026708415235.

Harrison, R.G., Carslaw, K.S., 2003. Ion aerosol cloud processes in the lower atmosphere. Reviews of Geophysics 41, 1012, http://dx.doi.org/10.1029/2002RG000114.

Harrison, R.G., Ambaum, M.H.P., 2008. Enhancement of cloud formation by droplet charging. Proceedings of the Royal Society A 464, 2561–2573, http://dx.doi.org/10.1098/rspa.2008.0009.

Hiremath, K.M., 2006. The influence of solar activity on the rainfall over India:cycle-to-cycle variations. Journal of Astrophysics and Astronomy 27, 367–372, http://dx.doi.org/%2010.1007/BF02702543.

Hoppel, W.A., Frick, G.M., 1986. Ion-aerosol attachment coefficients and the steady-state charge on aerosols in a bipolar ion environment. Aerosol Science and Technology 5, 1–21, http://dx.doi.org/10.1080/02786828608959073.

Jacobson, M.Z., 1999. Fundamentals of atmospheric modeling. Cambridge University Press.

Jacobson, M.Z., 2002. Analysis of aerosol interactions with numerical techniques for solving coagulation, nucleation, condensation, dissolution, and reversible chemistry among multiple size distribution. Journal of Geophysical Research 107 (D19), 4366, http://dx.doi.org/10.1029/2001JD002044.

Janssen, R.H., Ganzeveld, L.N., Kabat, P., Kulmala, M., Neiminen, T., Roebeling, R.A., 2011. Estimating seasonal variations in cloud droplet number concentrations over the boreal forest from satellite observations. Atmospheric Chemistry and Physics 11, 7701–7713.

Kanawade, V., Tripathi, S.N., 2006. Evidence for the role of ion-induced particle formation during an atmospheric nucleation event observed in Tropospheric Ozone Production about the Spring Equinox (TOPSE). Journal of Geophysical Research 111 (D2), D02209, http://dx.doi.org/1029/2005JD006366.

Kirkby, J., et al., 2011. Role of sulphuric acid, ammonia and galactic cosmic rays in atmospheric aerosol nucleation. Nature 476, 430, http://dx.doi.org/10.1038/nature10343.

Kulmala, M., Vehkamaki, H., Petaja, T., Maso, M.D., Lauri, A., Kerminen, V.-M., Birmili, W., McMurry, P.H., 2004. Formation and growth rates of ultrafne atmospheric particles: a review of observations. Aerosol Science 35, 143–176, http://dx.doi.org/10.1016/j.jaerosci.2003.10.003.

MacGorman, D.R., Rust, W.D., 1998. The electrical natureof storms. Oxford University Press, Oxford.

Martin, G.M., Johnson, D.W., Spcice, A., 1994. The measurement and parameterization of effective radius of droplets in warm stratocumulus clouds. Journal of the Atmospheric Sciences 51, 1823–1842.

Michael, M., Tripathi, S.N., Mishra, S.K., 2008. Dust charging and electrical conductivity in the day and night-time atmosphere of Mars. Journal of Geophysical Research 113, E07010, http://dx.doi.org/10.1029/2007JE003047.

Michael, M., Tripathi, S.N., Borucki, W.J, Whitten, R.C., 2009. Highly charging of particles by ion attachment in the atmosphere of Venus. Journal of Geophysical Research 114, EO4008, http://dx.doi.org/10.1029/2008JE003258.

Nenes, A., Ghan, S., Abdul-Razzak, H., Chuang, P.Y., Seinfeld, J.H., 2001. Kinetic limitations on cloud droplet formation and impact on cloud albedo. Tellus B 53, 133–149, http://dx.doi.org/10.1034/j.1600-0889.2001.d01-12.x.

Nicoll, K.A., Harrison, R.G., 2010. Experimental determination of layer cloud edge charging from cosmic ray ionisation. Geophysical Research Letters 37, L13802http://dx.doi.org/%2010.1029/2010GL043605.

O'Brien, K., 2005.The theory of cosmic-ray and high-energy solar particle transport in the atmosphere.The natural radiation environment VII, edited by: McLaughlin, J. P.

Renard, J.-B., Brogniez, C., Berthet, G., et al., 2008. Vertical distribution of the different types of aerosols in the stratosphere: detection of solid particles and analysis of their spatial variability. Journal of Geophysical Research 113, D21303, http://dx.doi.org/%2010.1029/2008JD010150.

Renard, J.-B., Berthet, G., Salazar, V., Catoire, V., Tagger, M., Gaubicher, B., Roberts, C., 2010. In situ detection of aerosol layers in the middle stratosphere. Geophysical Research Letters 37, L20803, http://dx.doi.org/10.1029/2010GL044307.

Renard, Tripathi, Michael, Rawal, Berthet, Fullekrug, Harrison, Robert, Tagger and Gaubicher, In situ detection of electrified aerosols in the upper troposphere and in the stratosphere,,Atmospheric Chemistry and Physics Discussions, Volume 13, Issue 3, 2013, pp.7061–7079 http://dx.doi.org/10.5194/acpd-13-7061-2013.

Rycroft M.J., Nicoll K.A., Aplin K.L., Harrison R.G., 2012. Recent advances in global electric circuit coupling between the space environment and the troposphere. Journal of Atmospheric and Solar-Terrestrial Physics 90-91, 198, http://dx.doi.org/10.1016/j.jastp.2012.03.015.

Seinfeld, J.H., Pandis, S.N., 2006. Atmospheric Chemistry and Physics—From Air Pollution to Climate Change, 2nd Edition John Wiley & Sons, Hoboken, New Jersey.

Srivastava, A.K., Tripathi, S.N., 2010. Numerical study for production of space charge within the stratiform cloud. Journal of Earth System Science 119 (5), 627–638, http://dx.doi.org/10.1007/s12040-010-0053-2.

Tinsley, B.A., Zhou, L., 2006. Initial results of a global circuit model with variable stratospheric and tropospheric aerosols. Journal of Geophysical Research 111, D16205, http://dx.doi.org/10.1029/2005JD006988.

Tinsley, B.A., Rohrbaugh, R.P., Hei, M., Beard, K.V., 2000. Effects of image charge on the scavenging of aerosol particles by cloud droplets, and on droplet charging and possible ice nucleation processes. Journal of the Atmospheric Sciences 57, 2118–2134, http://dx.doi.org/10.1175/1520-0469(2000)057%3c2118:EOICOT%3e2.0.CO;2.

Tinsley, B.A., Zhou, L., Plemmons, A., 2006. Changes in scavenging of particles by droplets due to weak electrification in clouds. Atmospheric Research 78, 266–295, http://dx.doi.org/10.1016/j.atmosres.2005.06.004.

Tripathi, S.N., Vishnoi, S., Kumar, S., Harrison, R.G., 2006. Computationally efficient expressions for the collision efficiency between electrically charged aerosol particles and cloud droplets. Quarterly Journal of the Royal Meterological Society 132, 1717–1731, http://dx.doi.org/10.1256/qj.05.125.

Tripathi, S.N., Harrison, R.G., 2001. Scavenging of electrified radioactive aerosols. Atmospheric Environment 35, 5817–5821.

Tripathi, S.N., Harrison, R.G., 2002. Enhancement of contact ice nucleation by scavenging of charged aerosol particles. Atmospheric Research 62, 57–70.

Tripathi, S.N., Michael, M., Harrison, R.G., 2008. Profiles of ion and aerosol interactions in planetary atmospheres. Space Science Reviews 137, 193–211, http://dx.doi.org/10.1007/s11214-008-9367-7.

Yu, F., Turco, R.P., 2001. From molecular clusters to nanoparticles: The role of ambient ionization in tropospheric aerosol formation. Journal of Geophysical Research 106, 4797–4814, http://dx.doi.org/10.1029/2000JD900539.

Zhou, L., Tinsley, B.A., 2007. The production of space charge at the boundaries of layer clouds. Journal of Geophysical Research 112, D11203, http://dx.doi.org/%2010.1029/2006JD007998.

Zhou, L., Tinsley, B.A., Plemmons, A., 2009. Scavenging in weakly electrified saturated and subsaturated clouds, treating aerosol particles and droplets as conducting spheres. Journal of Geophysical Research 114, D18201, http://dx.doi.org/10.1029/2008JD011527.

Zhau, J., Turco, R., Toon, B., 1995. A model simulation of pinatubo volcanic aerosols in the stratosphere. Journal of Geophysical Research 100, D4, http://dx.doi.org/%2010.1029/94JD03325.

Zaizen, Y., Ikegami, M., Okada, K., Makino, Y., 1995. Aerosol concentration observed at Zhangye in China. Journal of Meteorological Society of Japan 73, 891–897.